Reactivity of Isobutane on Zeolites: A First Principles Study

Xiaobo Zheng and Paul Blowers*

Department of Chemical and Environmental Engineering, The University of Arizona, P.O. Box 210011, Tucson, Arizona 85721-0011

Received: November 19, 2005; In Final Form: January 5, 2006

In this work, ab initio and density functional theory methods are used to study isobutane protolytic cracking, primary hydrogen exchange, tertiary hydrogen exchange, and dehydrogenation reactions catalyzed by zeolites. The reactants, products, and transition-state structures are optimized at the B3LYP/6-31G* level, and the final energies are calculated using the CBS-QB3 composite energy method. The computed activation barriers are 52.3 kcal/mol for cracking, 29.4 kcal/mol for primary hydrogen exchange, 29.9 kcal/mol for tertiary hydrogen exchange, and 59.4 kcal/mol for dehydrogenation. The zeolite acidity effects on the reaction barriers are also investigated by changing the cluster terminal Si−H bond lengths. The analytical expressions between activation barriers and zeolite deprotonation energies for each reaction are proposed so that accurate activation barriers can be obtained when using different zeolites as catalysts.

1. Introduction

Zeolites are commercially important solid acid catalysts for oil and petrochemical processes.[1] Particularly, the H-ZSM-5 zeolite is broadly used in the petrochemical industry for catalytic cracking of hydrocarbons because of its interesting catalytic properties, including shape selectivity and high acid strength.[2] Zeolites are crystalline aluminosilicates with three-dimensional framework structures that form uniformly sized pores of molecular dimension. It is well-known that zeolites are good catalysts because of their Brønsted acidic sites. These sites are formed when a silicon atom, which has a formal valency of four, is replaced by an aluminum atom with a valency of three. Because of the considerable covalency of the SiO and AlO bonds, a proton is attached to the oxygen atom connecting the silicon and its aluminum atom neighbor, resulting in a chemically stable structure, Si(OH)Al, where the oxygen atom becomes a three-coordinated structure. The "onium" type coordination of oxygen is the fundamental reason for the high acidity of the attached proton, which makes a zeolite a good catalyst.[3]

The conversion reactions of hydrocarbons by zeolite acid catalysts are essential for the modern oil and chemical industries.[4,5] Some researchers have reported experimental studies of hydrocarbon reactions.[6−11] However, because of the complicated reaction mechanisms and various simultaneous reaction pathways,[12,13] only limited information is available, and sometimes great differences lie between the experimental values, especially when different reactor types are utilized.[14]

On the other hand, in the past decade, the dramatic increase of computer speed has greatly increased the ability to apply computational tools for investigating large systems, including hydrocarbon reactions catalyzed by zeolites.[15−24] In this work, ab initio and density functional theory methods are applied to investigate isobutane reactions on zeolites. A T3 cluster, $H_3SiOAl(OH)SiH_3$, is used to simulate the zeolite surface where isobutane protolytic cracking, primary hydrogen exchange, tertiary hydrogen exchange, and dehydrogenation reactions will be studied. The results are then compared with those from experiment and previous computational research.

* Corresponding author. Tel.: 1-520-626-5319. Fax: 1-520-621-6048. E-mail: blowers@engr.arizona.edu.

2. Computational Methods

All of the calculations in this work were performed with the GAUSSIAN98 software package.[25] The geometries were optimized at the B3LYP/6-31G* level and the energies were obtained using CBS-QB3,[26] a complete basis set composite energy method. All products and reactants were verified with frequency calculations to be stable structures and all transition states were found to be first-order saddle points with only one negative eigenvalue. Additionally, intrinsic reaction coordinate (IRC) calculations showed that each reaction linked the correct products with reactants. Zero-point vibrational energies (ZPVE) were obtained from harmonic vibrational frequencies calculated at the B3LYP/6-31G* level with a scaling factor of 0.9806.[27]

3. Results and Discussions

3.1. Protolytic Cracking Reaction. The isobutane protolytic cracking reaction consists of the carbon−carbon bond cleavage of isobutane by the zeolite Brønsted acid proton, leading to the formation of methane and a surface sec-propyl alkoxide product, as shown in the reaction scheme below.

$$CH_3CH(CH_3)_2 + H_3SiOAlH_2(OH)SiH_3 \rightarrow CH_4 + H_3Si(OC_3H_7)AlH_2OSiH_3$$

The calculated transition-state structure using the B3LYP/6-31G* method is shown in Figure 1a. The C_4H_{11} fragment has a Mulliken charge of +0.804, which makes it similar to the nonclassical $C_4H_{11}^+$ carbonium ion. In the transition-state structure, the C(15)−C(16) distance is greatly extended from 1.54 Å in isobutane to 2.00 Å, indicating the bond rupture mode. The acidic proton moves away from the zeolite cluster and the H(14)−O(3) distance reaches 1.91 Å compared with 0.98 Å

10.1021/jp056707v CCC: $33.50
Published on Web 02/02/2006

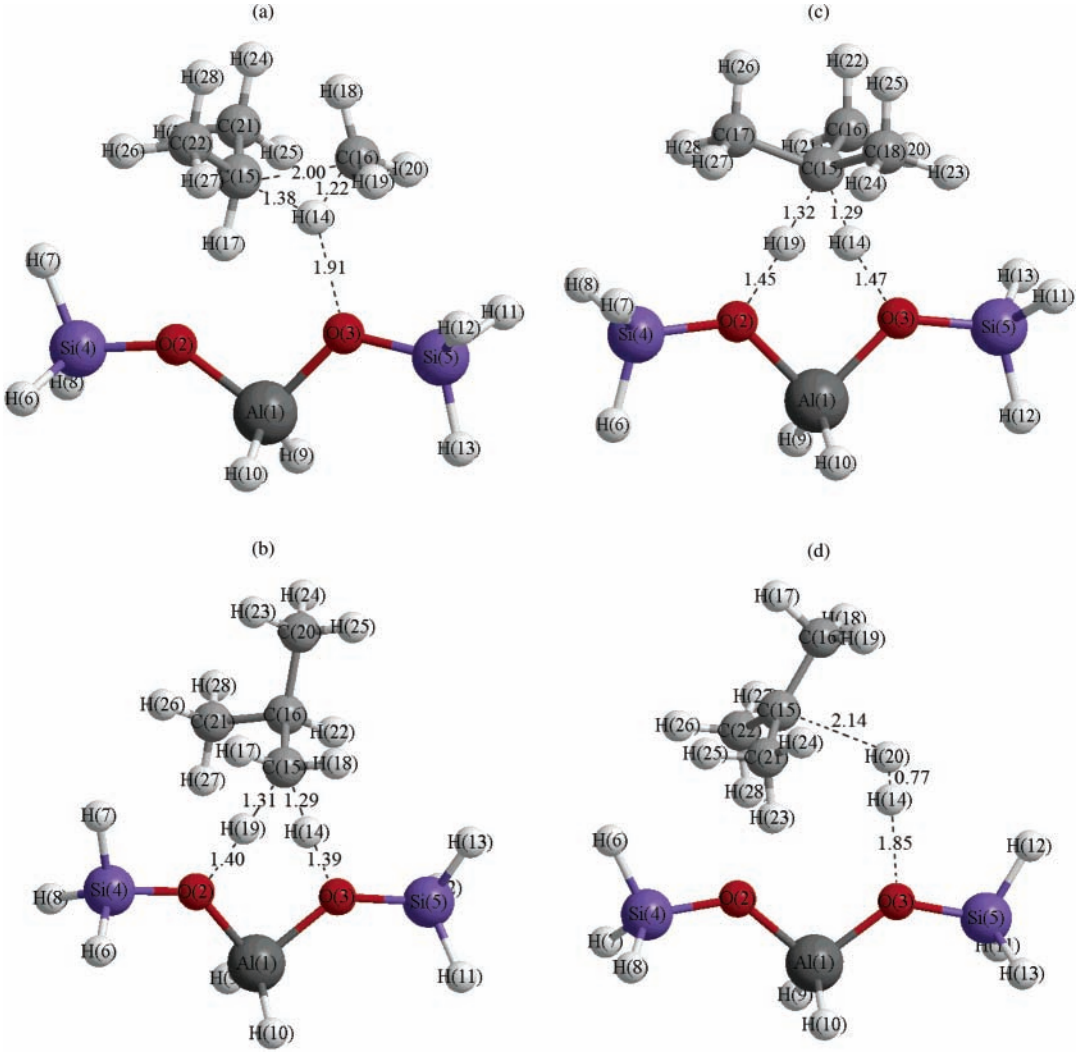

Figure 1. Transition-state structures for isobutane reactions on a zeolite cluster: (a) cracking reaction, (b) primary hydrogen exchange reaction, (c) tertiary hydrogen exchange reaction, (d) dehydrogenation reaction (units in Å).

for the zeolite-free cluster. The H(14)−C(16) distance is 1.22 Å, which is approaching that of the methane product, 1.09 Å. The isopropyl fragment, C_3H_7, is bonded to the zeolite oxygen, O(2), and forms a surface alkoxide.

The zeolite cluster plays an important role in this reaction. The right oxygen of the cluster, O(3), acts as a Brønsted acid that donates a proton, while the left oxygen, O(2), acts as a Lewis base that receives the propyl group. This transition-state structure demonstrates the typical bifunctional Brønsted acidic−Lewis basic nature of the zeolite catalyst.

The activation barrier for this protolytic reaction obtained with the CBS-QB3 method is 52.3 kcal/mol. It is much lower than those of other reactions from this research group using a similar methodology−71.4 kcal/mol for ethane[28] and 62.1 kcal/mol for propane.[29] This indicates that the alkane protolytic reactions take place more easily as the carbon chain length increases from C2 to C3 and C4.

The barrier calculated in work is compared with the previous computational results and available experimental data in Table 1. Kazansky reported an activation barrier of 57.5 kcal/mol using the MP2/6-31++G**//HF/6-31G* (energy calculation method//geometry optimization method) and a small T1 zeolite cluster.[30] The barrier is relatively higher than that of this work because the small T1 cluster used is unable to include the important long-range interactions of the zeolite catalyst and MP2 energy calculations tend to overestimate barrier heights.[31−34] With a T3 cluster, Rigby studied the reaction using the MP2/6-31G*//HF/3-21G method, and the activation barrier obtained is even higher, 68.0 kcal/mol. Furthermore, several research groups conducted experimental studies of this reaction. The reported experimental activation energies are 29.0 kcal/mol from Sun[10] and 29.9 kcal/mol from Narbeshuber[8] using H−ZSM-5 zeolite as the catalyst. Corma et al. reported an activation energy of 37.5 and 40.6 kcal/mol using the USY zeolite with different Si/O ratios.[35] The apparent experimental activation energy obtained by Stefanadis is 57.0 kcal/mol. Since the experimental adsorption energy of isobutane on zeolites is in the range from 10 to 15 kcal/mol,[8] the activation energy from Stefanadis is calculated to be 42−47 kcal/mol. It can be found that the experimental results vary greatly from a low value of 29.0 kcal/mol to a much higher value of 47.0 kcal/mol. The great difference in the experimental values highlights the difficulty in measuring activation energies, especially when different reactor types are utilized.[14] Also, the experimental results may depend on the isobutane surface coverage ratio, Si/Al ratio, and temperature. The calculated activation barrier from this work is slightly higher than the experimental data from Stefanadis and has better agreement than the computational works of Kanzansy and Rigby compared with the experimental results.

3.2. Hydrogen Exchange Reactions. The isobutane hydrogen exchange reactions can take place at either the primary carbon

TABLE 1: Activation Barrier Calculation Results for Isobutane Conversion Reactions on Zeolites Compared with Previous Computational and Experimental Studies

	this work	Kanzansky[30]	Rigby[49]	Esteves[36]	Furtado[38]
cluster model	T3	T1	T3	T3	T5
geometry optimization method	B3LYP/6-31G*	HF/6-31G*	HF/3-21G	B3LYP/6-31G**	B3LYP/6-311G**
energy calculation method	CBS-QB3	MP2/6-31++G**	MP2/6-31G*	B3LYP/6-31G**	B3LYP/6-311G**
cracking	52.3	57.5	68.0	–	–
primary H-exchange	29.4	–	–	32.3	–
tertiary H-exchange	29.9	–	–	36.2	–
dehydrogenation	59.4	66.9, 74.7	–	–	53.5

	this work	Stefanadis[7]	Sun[50]	Narbeshuber[8,9]	Corma[35]
zeolite catalyst type		H-ZSM-5	H-ZSM-5	H-ZSM-5	USY
cracking	52.3	57.0 (apparent)	29.0 ± 0.4	29.9	40.6 ± 0.4, 37.5 ± 4.5
primary H-exchange	29.4	–	–	–	–
tertiary H-exchange	29.9	–	–	–	–
dehydrogenation	59.4	–	29.5 ± 0.3	23.9	28.0 ± 0.6, 39.6 ± 5.3

or the tertiary carbon, as shown in the reaction scheme below.

$$C\mathrm{H_3CH(CH_3)_2} + \mathrm{H_3SiOAlH_2(OH')SiH_3} \rightarrow C\mathrm{H_2H'CH(CH_3)_2} + \mathrm{H_3Si(OH)AlH_2OSiH_3}$$

$$\mathrm{CH_3}C\mathrm{H(CH_3)_2} + \mathrm{H_3SiOAlH_2(OH')SiH_3} \rightarrow \mathrm{CH_3}C\mathrm{H'(CH_3)_2} + \mathrm{H_3Si(OH)AlH_2OSiH_3}$$

The italic carbon atom indicates the place where the hydrogen exchange takes place. Figure 1b shows the calculated transition-state structure for the primary hydrogen exchange reaction of isobutane optimized at the B3LYP/6-31G* level. The carbon in the main plane of the zeolite structure, C(15), is protonated and becomes a pentacoordinated structure. The exchanging hydrogen, H(19), and the acidic proton, H(14), stay in the middle of the carbon and two oxygen atoms, (O2) and (O3), indicating the formation of one C−H bond and breaking of the other. The right oxygen of the cluster, O(3), acts as a Brønsted acid that donates a proton. The left oxygen, (O2), acts as a Lewis base that receives the hydrogen atom from isobutane.

The activation barrier obtained with the CBS-QB3 method is 29.4 kcal/mol as listed in Table 1. Esteves et al. studied this reaction using the B3LYP/6-31G**//B3LYP/6-31G** method and a T3 cluster.[36] The activation barrier reported is 32.3 kcal/mol, relatively higher than our value. Unfortunately, there is no experimental data to compare with directly. Stepanov reported the experimental activation energy of 25.8 ± 1.7 kcal/mol for the propane primary hydrogen exchange reaction.[37] Considering the fact that the isobutane hydrogen exchange should be similar to propane, our calculated activation barrier is expected to be reliable.

Figure 1c is the transition-state structure for the isobutane tertiary hydrogen exchange reaction optimized at B3LYP/6-31G* level. The hydrogen exchange reaction takes place at the center carbon, C(15), which is protonated and becomes a pentacoordinated structure. The C(16)−C(17)−C(18) plane becomes almost flat and perpendicular to the main cluster plane, O(2)−Al(1)−O(3). The exchanging hydrogen, H(19), and the acidic hydrogen, H(14), stay in the middle of the carbon and two oxygen atoms, (O2) and (O3), indicating formation of one C−H bond and breaking of the other.

The activation barrier obtained with the CBS-QB3 method is 29.9 kcal/mol, which is similar to but slightly higher than that of the primary hydrogen exchange. Esteves reported a relatively higher barrier of 36.2 kcal/mol for this reaction using the B3LYP/6-31G**//B3LYP/6-31G** method and a T3 cluster. Again, there is no reported experimental study for this reaction. Considering that the experimental activation energy of the propane secondary hydrogen exchange is 28.0 ± 1.7 kcal/mol,[37] our calculated result agrees well with it.

3.3. Dehydrogenation Reaction. For dehydrogenation, only the hydrogen attached to the tertiary carbon is available for attack by acidic zeolite sites,[10] as shown in the reaction scheme below.

$$\mathrm{CH_3CH(CH_3)_2} + \mathrm{H_3SiOAlH_2(OH)SiH_3} \rightarrow \mathrm{H_2} + \mathrm{H_3Si(OC_4H_9)AlH_2OSiH_3}$$

The dehydrogenation reaction consists of cleavage of a carbon−hydrogen bond by the zeolite Brønsted acid proton. The optimized transition-state structure at the B3LYP/6-31G* level is shown in Figure 1d. The carbon structure, C(15)−C(16)−C(21)−C(22), becomes almost planar, and a six-membered ring, O(2)−Al(1)−O(3)−H(14)−H(20)−C(15), is formed. The H(20)−C(15) distance is greatly extended from 1.07 Å in isobutane to 2.14 Å, indicating the bond-breaking mode. The acidic proton, H(14), moves away from the zeolite cluster and the H(14)−O(3) distance reaches 1.85 Å compared with 0.98 Å for the zeolite free cluster. Meanwhile, these two hydrogens move closer to each other and a dihydrogen molecule is almost formed with a distance of 0.77 Å.

The activation barrier obtained with the CBS-QB3 method is 59.4 kcal/mol. This barrier is the highest among the four isobutane conversion reactions, indicating it is the most difficult reaction to take place. Compared with other researchers' computational work, this barrier is slightly higher than the result obtained by Furtado[38] using the B3LYP/6-311G**//B3LYP/6-311G** method and a T5 cluster and much less than the results obtained by Kazansky, 66.9 and 74.7 kcal/mol, using the MP2/6-31++G**//HF/6-31G* method and a T1 cluster.[30] Several research groups have reported experimental studies of this reaction, and the activation energies vary from the low value of 23.0 kcal/mol by Narbeshuber [9] to the high value of 39.6 ± 5.3 kcal/mol by Croma.[35] This discrepancy between the computational results and the experimental values could be caused by the limited size of the zeolite cluster used in the computational works, since the T3 and T5 cluster cannot include the long-range interactions of the zeolite catalyst and could lead to the overestimation of barrier heights.[14] Zygmunt included the long-range correction for the ethane protolytic cracking reaction recently,[39] which was obtained with a HF/6-31G* correction for the 58T cluster model. This correction reduces the activation barrier by 14.50 kcal/mol. For the same scenario, the long-range correction could also lower our calculated barrier height and bring it much closer to the experimental value.

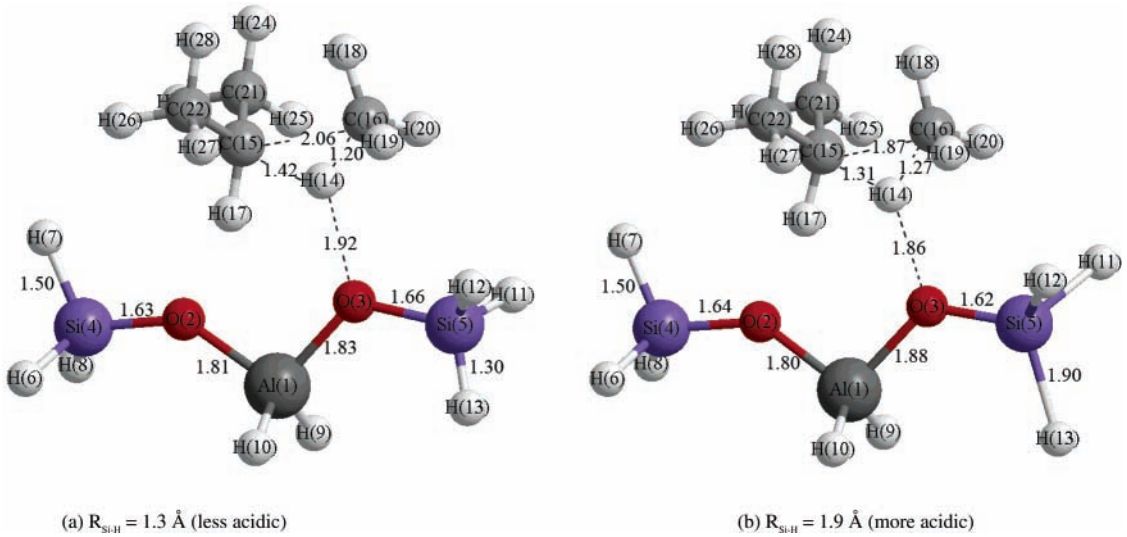

Figure 2. Transition-state structures of isobutane cracking reaction with changing terminal Si−H bond distances (units in Å).

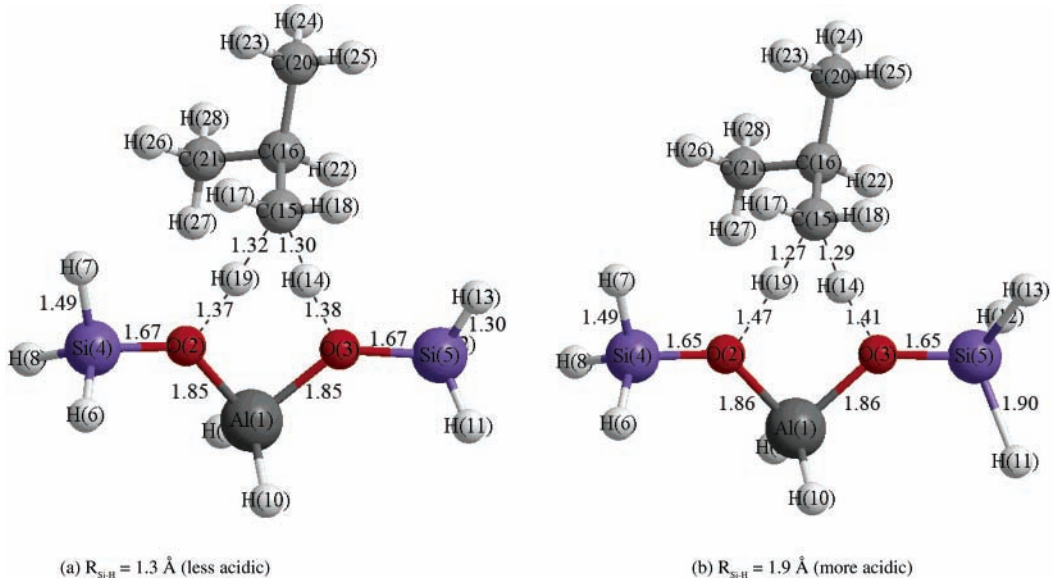

Figure 3. Transition-state structures of isobutane primary hydrogen exchange reaction with changing terminal Si−H bond distances (units in Å).

Moreover, zeolite acidic effects could also reduce our calculated activation barrier by an additional 1.5 kcal/mol, which will be discussed in the next section.

From the discussion above, the reactivity sequence found for zeolite catalytic reactions of isobutane is:

dehydrogenation < protolytic cracking < hydrogen exchange
(59 kcal/mol) (52 kcal/mol) (29 kcal/mol)

3.4. Acidity Effects. The acidity effect study of zeolite catalysts is important since the zeolite acidity is directly related to the strength of the acid sites.[40] It has been shown by Kramer et al.[41,42] that the acidity effect of zeolite catalysts can be simulated by modifying the peripheral bonds of the cluster model. The deprotonation energy is a theoretical measurement of zeolite acidity and it is a good indication of a cluster's chemical properties. In a zeolite cluster, the deprotonation energy (E_{dep}) is defined as the energy difference between the protonated (ZH) and unprotonated (Z^-) clusters:[43]

$$E_{dep} = E(Z^-) - E(ZH)$$

In real zeolite catalysts, the deprotonation energy varies over the range from 20 to 50 kcal/mol among different zeolite structures. This can be mimicked by assigning different bond lengths to the terminal Si−H bonds of the cluster with all other geometry parameters optimized.

Assigning the terminal Si−H bond lengths to a value less than its equilibrium value, 1.47 Å, decreases the acidity, and the deprotonation energy increases. Similarly, increasing the terminal Si−H bond length will increase the acidity, and the deprotonation energy decreases. As a result, the acidic proton becomes more active and the reaction is facilitated. The changes in the zeolite acidity also affect the transition-state structures and activation barriers of the reactions. Figure 2 shows the transition-state structures of the isobutane protolytic cracking reaction as the terminal Si−H distance changes from 1.3 to 1.9 Å. The acidic proton and oxygen distance, H(14)−O(3), decreases from 1.92 to 1.86 Å as the cluster acidity increases. Meanwhile, the C(15)−C(16) distance decreases from 2.06 to 1.87 Å and the H(14)−C(16) distance slightly increases from 1.20 to 1.27 Å. Similar acidic studies were applied to isobutane primary and tertiary hydrogen exchange reactions, and the transition-state structures are shown in Figures 3 and 4. In

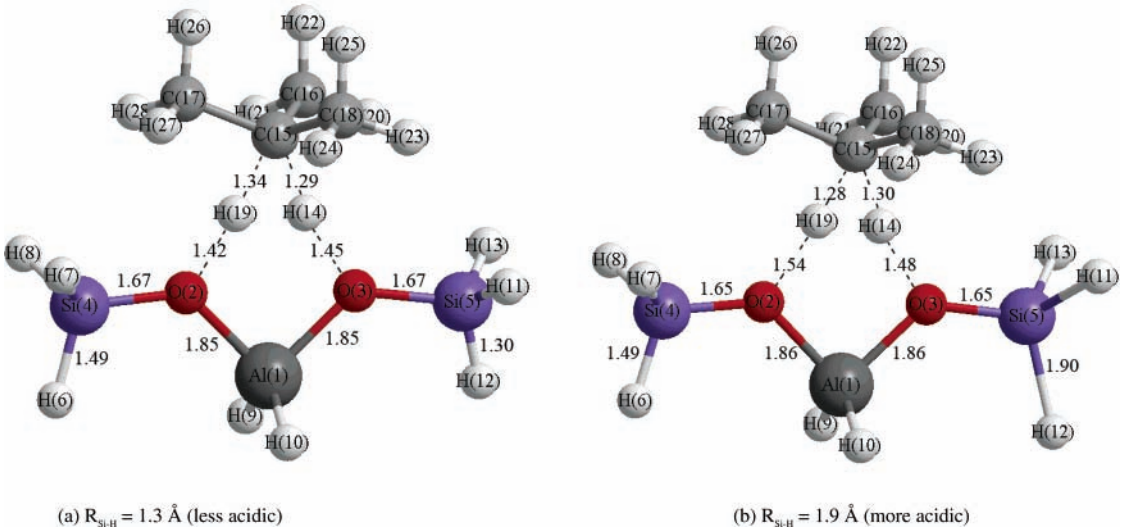

Figure 4. Transition-state structures of isobutane tertiary hydrogen exchange reaction with changing terminal Si−H bond distances (units in Å).

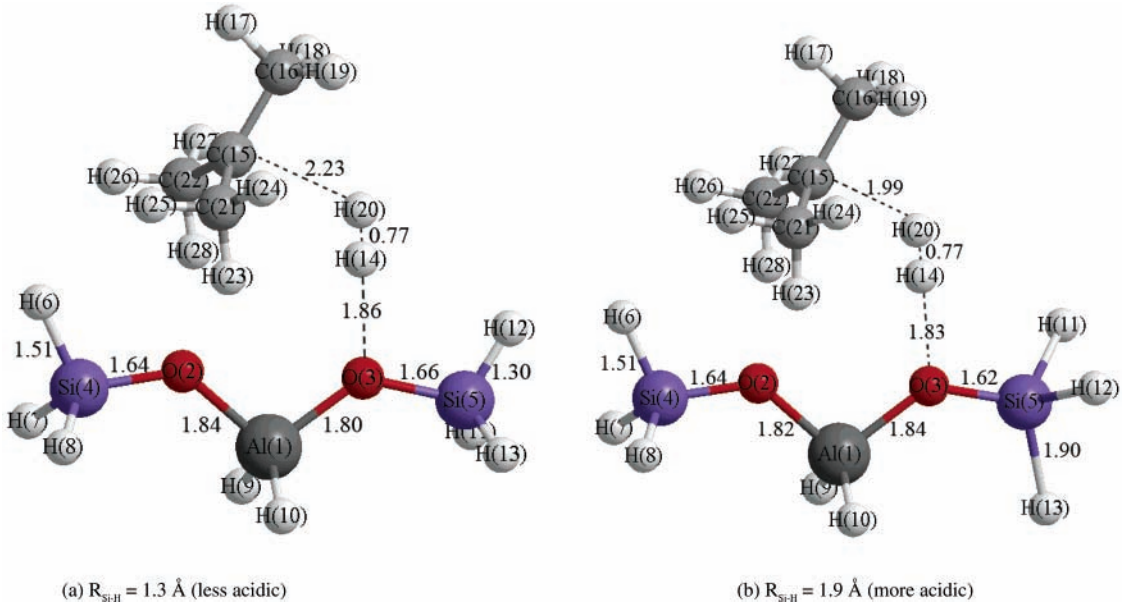

Figure 5. Transition-state structures of isobutane dehydrogenation reaction with changing terminal Si−H bond distances (units in Å).

TABLE 2: Effects of Si−H Distances on Activation Barriers (units in kcal/mol)

	activation barrier (E_a)				
	cracking	primary H-exchange	tertiary H-exchange	dehydrogenation	deprotonation energy (E_{dep})
R_{Si-H} = 1.30 Å	56.7	31.8	32.4	62.9	304.0
R_{Si-H} = 1.47 Å	52.3	29.4	29.9	59.4	297.9
R_{Si-H} = 1.70 Å	47.3	26.7	26.8	55.5	291.6
R_{Si-H} = 1.90 Å	43.4	24.6	24.6	52.5	285.8
HZSM-5	50.3	28.3	28.7	57.9	295.4
relationship	$E_a = 0.737E_{dep} - 167.3$	$E_a = 0.391E_{dep} - 87.1$	$E_a = 0.435E_{dep} - 99.8$	$E_a = 0.577E_{dep} - 112.4$	

hydrogen exchange reactions, as the terminal Si−H distance increases from 1.3 to 1.9 Å, the acidic proton and oxygen distance, H(14)−O(3), increases and the exchange hydrogen and oxygen distance, H(19)−O(2), increases as well. Meanwhile, the C_4H_{11} fragment moves away from the zeolite cluster. The transition-state structures of the isobutane dehydrogenation reaction as the Si−H distance changes to 1.3 and 1.9 Å are shown in Figure 5. The acidic proton and oxygen distance, H(14)−O(3), decreases slightly from 1.86 to 1.83 Å and the H(20)−C(15) distance decreases from 2.23 to 1.99 Å. Meanwhile, the H(14)−H(20) distance increases slightly from 0.768 to 0.772 Å.

The changes in activation barriers for isobutane cracking, dehydrogenation, and hydrogen exchange reactions as the Si−H bond distances vary are listed in Table 2. With an increase in the Si−H distance, the activation barriers decrease for all four reactions, because of the increased acidity of the zeolite cluster. Applying the Brønsted−Polanyi principle, the following relationship can be used:[13]

$$\Delta E_a = c\Delta E_{dep} \text{ or } E_a = c\Delta E_{dep} + b$$

As long as the reaction mechanism does not alter, the change in activation energy is linearly correlated to the change in

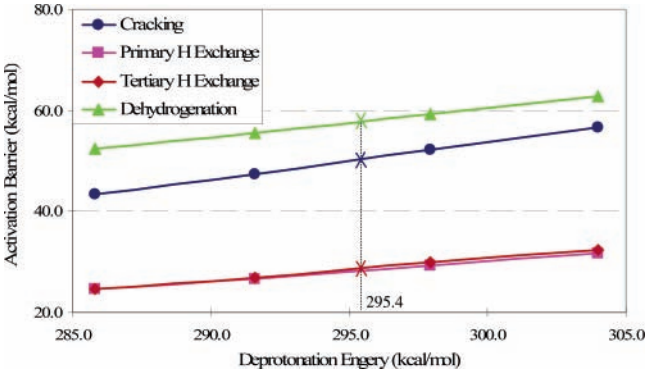

Figure 6. Correlations of the calculated isobutane conversion reactions activation barriers to the acidity effects represented by deprotonation energies.

deprotonation energy for each reaction. The relationships of the activation barriers with cluster deprotonation energies are illustrated in Figure 6. The slopes of primary and tertiary hydrogen exchange reactions are similar, which are different from those of the cracking and dehydrogenation reactions. This indicates the different mechanistic dependence of activation barriers on deprotonation energies for cracking, hydrogen exchange, and dehydrogenation reactions.

For zeolite type H-ZSM-5, the deprotonation energy of 295.4 kcal/mol[43−47] has now been widely accepted.[29,39,48] Applying this deprotonation energy, the activation barriers are then calculated using the correlations listed in Table 2. With the acidity effects, the activation barriers of the isobutane protolytic cracking, primary hydrogen exchange, tertiary hydrogen exchange, and dehydrogenation reactions are lowered by 2.0, 1.1, 1.2, and 1.5 kcal/mol, which bring our calculated values closer to the experimental results.

With the correlations between the deprotonation energy and activation barrier for isobutane conversion reactions, activation barriers can be obtained for different zeolite catalysts without performing the difficult transition-state optimizations as long as the zeolite deprotonation energies are first acquired. Since the calculations to get the deprotonation energy are much easier to conduct, the prediction of activation barriers could become easier for these reactions on other zeolites by using the correlations.

Acknowledgment. This work was funded by the State of Arizona through the Office of the Vice President for Research at the University of Arizona. Supercomputer time was provided by the National Computational Science Alliance and used the NCSA HP/Convex Exemplar SPP-2000 at the University of Illinois at Urbana−Champaign.

References and Notes

(1) Maesen, T.; Marcus, B. *Stud. Surf. Sci. Catal.* **2001**, *137 (Introduction to Zeolite Science and Practice, 2nd ed.)*, 1.

(2) McCusker, L. B.; Baerlocher, C. *Stud. Surf. Sci. Catal.* **2001**, *137 (Introduction to Zeolite Science and Practice, 2nd ed.)*, 37.

(3) Flanigen, E. M. *Stud. Surf. Sci. Catal.* **2001**, *137 (Introduction to Zeolite Science and Practice, 2nd ed.)*, 11.

(4) Wojciechowski, B. W.; Corma, A. *Catalytic Cracking: Catalysts, Chemistry, and Kinetics*; Dekker: New York, 1986.

(5) Maxwell, I. E.; Stork, W. H. J. *Stud. Surf. Sci. Catal.* **2001**, *137 (Introduction to Zeolite Science and Practice 2nd ed.)*, 747.

(6) Makarova, M. A.; Ojo, A. F.; Karim, K.; Hunger, M.; Dwyer, J. *J. Phys. Chem.* **1994**, *98*, 3619.

(7) Stefanadis, C.; Gates, B. C.; Haag, W. O. *J. Mol. Catal.* **1991**, *67*, 363.

(8) Narbeshuber, T. F.; Vinek, H.; Lercher, J. A. *J. Catal.* **1995**, *157*, 388.

(9) Narbeshuber, T. F.; Brait, A.; Seshan, K.; Lercher, J. A. *J. Catal.* **1997**, *172*, 127.

(10) Sun, Y. P.; Brown, T. C. *J. Catal.* **2000**, *194*, 301.

(11) Bizreh, Y. W.; Gates, B. C. *J. Catal.* **1984**, *88*, 240.

(12) van Santen, R. A.; van de Graaf, B.; Smit, B. *Stud. Surf. Sci. Catal.* **2001**, *137 (Introduction to Zeolite Science and Practice, 2nd ed.)*, 419.

(13) van Santen, R. A.; Kramer, G. J. *Chem. Rev.* **1995**, *95*, 637.

(14) Curtiss, L. A.; Gordon, M. S. *Computational Materials Chemistry Methods and Applications*; Kluwer Academic Publishers: Dordrecht; Boston; London, 2004.

(15) Lynch, B. J.; Truhlar, D. G. *J. Phys. Chem. A* **2001**, *105*, 2936.

(16) Jursic, B. S. *J. Chem. Soc., Perkin Trans. 2* **1997**, 637.

(17) Truong, T. N.; Truong, T. T. T. *Chem. Phys. Lett.* **1999**, *314*, 529.

(18) Truong, T. N. *J. Chem. Phys.* **2000**, *113*, 4957.

(19) Blowers, P.; Masel, R. *AIChE J.* **2000**, *46*, 2041.

(20) Wong, M. W.; Radom, L. *J. Phys. Chem. A* **1998**, *102*, 2237.

(21) Wong, M. W.; Radom, L. *J. Phys. Chem.* **1995**, *99*, 8582.

(22) Wong, M. W.; Pross, A.; Radom, L. *J. Am. Chem. Soc.* **1994**, *116*, 6284.

(23) Xiao, Y. T.; Longo, J. M.; Hieshima, G. B.; Hill, R. J. *Ind. Eng. Chem. Res.* **1997**, *36*, 4033.

(24) Saeys, M.; Reyniers, M. F.; Marin, G. B. *J. Phys. Chem. A* **2003**, *107*, 9147.

(25) Frisch, M. J.; Trucks, G. W.; Schlegel, H. B.; Gill, P. M. W.; Johnson, B. G.; Robb, M. A.; Cheeseman, J. R.; Keith, T.; Petersson, G. A.; Montegomery, J. A.; Raghavachari, K.; Al-Laham, M. A.; Zakrzewski, V. G.; Ortiz, J. V.; Foresman, J. B.; Cioslowski, J.; Stefanov, B. B.; Nanayakkara, A.; Challacombe, M.; Peng, C. Y.; Ayala, P. Y.; Chen, W.; Wong, M. W.; Andres, J. L.; Replogle, E. S.; Gomperts, R.; Martin, R. L.; Fox, D. J.; Binkley, J. S.; Defrees, D. J.; Baker, J.; Stewart, J. P.; Head-Gordon, M.; Gonzalez, C.; Pople, J. A. *Gaussian 98*, Revision A.7; Gaussian, Inc.: Pittsburgh, PA, 1995.

(26) Montgomery, J. A.; Frisch, M. J.; Ochterski, J. W.; Petersson, G. A. *J. Chem. Phys.* **1999**, *110*, 2822.

(27) Scott, A. P.; Radom, L. *J. Phys. Chem.* **1996**, *100*, 16502.

(28) Zheng, X.; Blowers, P. *J. Mol. Catal. A* **2005**, *229*, 77.

(29) Zheng, X.; Blowers, P. *J. Phys. Chem. A* **2005**, *109*, 10734.

(30) Kazansky, V. B.; Frash, M. V.; vanSanten, R. A. *Appl. Catal. A* **1996**, *146*, 225.

(31) Willis, B. G.; Jensen, K. F. *J. Phys. Chem. A* **1998**, *102*, 2613.

(32) Lee, W. T.; Masel, R. I. *J. Phys. Chem.* **1996**, *100*, 10945.

(33) Lee, W. T.; Masel, R. I. *J. Phys. Chem.* **1995**, *99*, 9363.

(34) Yamataka, H.; Nagase, S.; Ando, T.; Hanafusa, T. *J. Am. Chem. Soc.* **1986**, *108*, 601.

(35) Corma, A.; Miguel, P. J.; Orchilles, A. V. *J. Catal.* **1994**, *145*, 171.

(36) Esteves, P. M.; Nascimento, M. A. C.; Mota, C. J. A. *J. Phys. Chem. B* **1999**, *103*, 10417.

(37) Stepanov, A. G.; Ernst, H.; Freude, D. *Catal. Lett.* **1998**, *54*, 1.

(38) Furtado, E. A.; Milas, I.; Lins, J.; Nascimento, M. A. C. *Phys. Status Solidi A* **2001**, *187*, 275.

(39) Zygmunt, S. A.; Curtiss, L. A.; Zapol, P.; Iton, L. E. *J. Phys. Chem. B* **2000**, *104*, 1944.

(40) Sillar, K.; Burk, P. *J. Mol. Struct.*—THEOCHEM **2002**, *589*, 281.

(41) Kramer, G. J.; Vansanten, R. A.; Emeis, C. A.; Nowak, A. K. *Nature* **1993**, *363*, 529.

(42) Evleth, E. M.; Kassab, E.; Sierra, L. R. *J. Phys. Chem.* **1994**, *98*, 1421.

(43) Brand, H. V.; Curtiss, L. A.; Iton, L. E. *J. Phys. Chem.* **1993**, *97*, 12773.

(44) Sauer, J.; Sierka, M. *J. Comput. Chem.* **2000**, *21*, 1470.

(45) Eichler, U.; Brandle, M.; Sauer, J. *J. Phys. Chem. B* **1997**, *101*, 10035.

(46) Datka, J.; Boczar, M.; Rymarowicz, P. *J. Catal.* **1988**, *114*, 368.

(47) Grau-Crespo, R.; Peralta, A. G.; Ruiz-Salvador, A. R.; Gomez, A.; Lopez-Cordero, R. *Phys. Chem. Chem. Phys.* **2000**, *2*, 5716.

(48) Frash, M. V.; van Santen, R. A. *Top. Catal.* **1999**, *9*, 191.

(49) Rigby, A. M.; Kramer, G. J.; vanSanten, R. A. *J. Catal.* **1997**, *170*, 1.

(50) Martin, J. M. L.; Sundermann, A.; Fast, P. L.; Truhlar, D. G. *J. Chem. Phys.* **2000**, *113*, 1348.